Single molecule study of the DNA denaturation phase transition in the force-torsion space

D. Salerno,[1] A. Tempestini,[1] I. Mai,[1] D. Brogioli,[1] R. Ziano,[1] V. Cassina,[1] and F. Mantegazza[1]

[1]Dipartimento di Medicina Sperimentale, Università degli Studi di Milano - Bicocca, Via Cadore 48, Monza (MB) 20900, Italy.

We use the "magnetic tweezers" technique to reveal the structural transitions that DNA undergoes in the force-torsion space. In particular, we focus on regions corresponding to negative supercoiling. These regions are characterized by the formation of so-called denaturation bubbles, which have an essential role in the replication and transcription of DNA. We experimentally map the region of the force-torsion space where the denaturation takes place. We observe that large fluctuations in DNA extension occur at one of the boundaries of this region, i.e., when the formation of denaturation bubbles and of plectonemes are competing. To describe the experiments, we introduce a suitable extension of the classical model. The model correctly describes the position of the denaturation regions, the transition boundaries, and the measured values of the DNA extension fluctuations.

The nanomechanics of DNA play an important role at the biological and biochemical levels [1]. Thus, understanding the transcription and duplication phenomena is a relevant open topic to which a quantitative comprehension of DNA mechanical characteristics is fundamental. In particular, because any transcription or duplication process implies the local and temporary separation of the two DNA strands (i.e., DNA breathing [2, 3] or denaturation bubbles [4–6]), understanding denaturation represents the first building block towards the theoretical comprehension of DNA metabolism. A well-known and promising technique for studying nanomechanical properties is the magnetic tweezers (MT), which allows one to impose a stretching force and a torsion to a single DNA molecule while also monitoring the simultaneous extension of the same molecule [7, 8]. The versatility of the MT technique has been exploited to investigate DNA nanomechanics in the presence of proteins, enzymes, ligands, and drugs [9–13], and phenomenologically analyzed [14]. The initial pioneering MT studies focused on the topology of DNA molecules and showed that torsion can produce a so-called "plectoneme", which reduces DNA extension [15, 16]. For modeling plectoneme formation, the DNA can be simply described as an elastic rod [17]. The experiments showed that the plectonemes disappear when the force becomes sufficiently high and the direction of the torsion is toward the unwinding of the DNA double helix [8]. This chiral effect, which goes beyond the elastic rod model, has been explained in terms of denaturation of the double helix [18].

In this work we use the asymmetry between the DNA extension under positive and negative torsion as a hallmark of denaturation. For the first time, we systematically evaluate the occurrence of mechanical denaturation in the force-torsion space. We find that large temporal fluctuations of extension arise at one of the boundaries of the denaturation region. Finally, we interpret the experimental data with a simple mechanical model obtained by considering a denaturation term to the classical energy [17] used to describe the buckling transition.

Several MT apparatuses have already been reported in the literature and, in our set up [12], we generally follow the most classically proposed schemes [8, 19]. The technique is based on the following procedure: one end of the DNA is connected by standard biochemical techniques [8] to a commercial micron-sized superparamagnetic bead and the other DNA end is fixed to the inner wall of a squared capillary tube [20, 21]. Forces or torsions are then applied to the bead through a field generated by external permanent magnets, whose position and rotation can be controlled [22, 23]. The movement of the magnetic bead is transferred to the DNA and thus, indirectly, forces or torsions are applied to the molecule [24]. The DNA extension L_e is measured by considering the diffraction images generated at different heights of the bead, which is illuminated by a LED light [19]. The force F exerted by the magnetic field on the bead and, as consequence exerted on the DNA, is obtained as in ref. [20].

Figure 1 shows the average value of the extension $\langle L_e \rangle$ of a DNA (~ 6000 base pairs) molecule as a function of the number of imposed turns n_t at different values of the applied stretching force ($F = 0.25$ pN, 0.63 pN, 0.79 pN, and 1.14 pN). The data are the result of an averaging procedure on several values of $L_e(t)$ taken as a function of time at a frequency rate of 60 Hz during a time interval of several seconds. These results are typical in the literature of MT [17] and are qualitatively described as follows. When increasing the absolute value of n_t, the torsion is first absorbed by elastic twist deformations and the DNA extension remains approximately constant. Above the so called n_b buckling transition, dependent on F and indicated by the vertical arrows in Fig. 1, the creation of plectonemes induces a progressive linear decrease in the DNA extension. At low forces ($F < 0.6$ pN), when increasing n_t, the data show a symmetric trend at positive
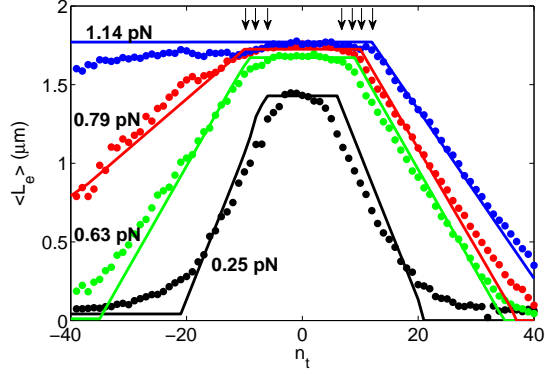
2

FIG. 1: Average DNA extension $\langle L_e \rangle$ as a function of the number of imposed turns n_t. Data (*dots*) and theoretical curves (*lines*) are obtained for different values of the applied force F, as indicated in the figure. The short vertical arrows point to the buckling transitions n_b.
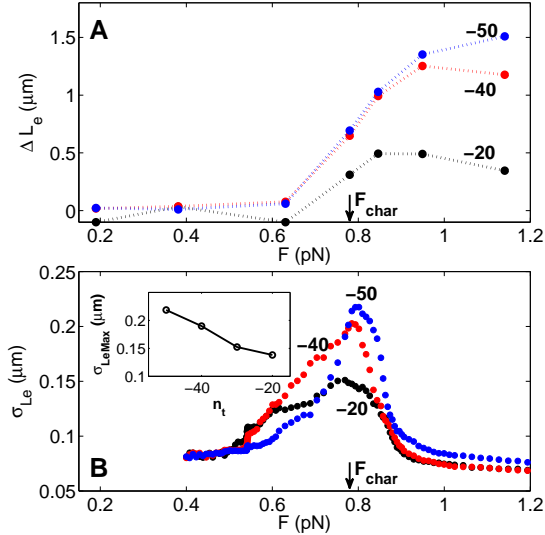

FIG. 2: Asymmetry $\Delta L_e(n_t) = \langle L_e(-n_t) \rangle - \langle L_e(n_t) \rangle$ (*Panel A*) and standard deviation of the DNA extension σ_{L_e} (*Panel B*). measured as a function of the applied force F. Data obtained for different values of the imposed turns n_t (indicated in the figures). Inset: measured maximum values $\sigma_{L_e Max}$ obtained from the σ_{L_e} vs F curves shown in the main figure.

and negative torsion. At high force values ($F > 1$ pN), the situation is different: at negative imposed turns, the L_e vs n_t curves are no longer symmetric, and the DNA extension is approximately constant due to the formation of so-called denaturation bubbles [18].

The asymmetric behavior of the $\langle L_e \rangle$ vs n_t is quantified by the expression $\Delta L_e(n_t) = \langle L_e(-n_t) \rangle - \langle L_e(n_t) \rangle$. The $\Delta L_e(n_t)$ values are shown in Fig. 2A as a function of F. We observe a transition between the plectonemic behavior at low forces and the formation of denaturation bubbles at high forces. This transition is highlighted by an increasing asymmetry and occurs around a character-
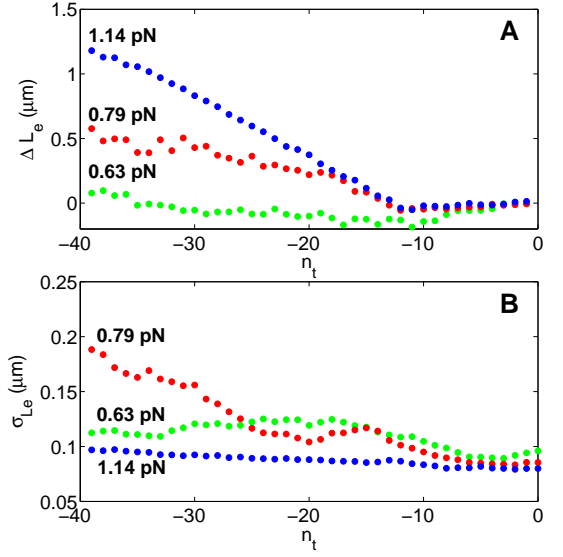

FIG. 3: Asymmetry $\Delta L_e(n_t) = \langle L_e(-n_t) \rangle - \langle L_e(n_t) \rangle$ (*Panel A*) and standard deviation of the DNA extension σ_{L_e} (*Panel B*) measured as a function of the imposed turns n_t. Data obtained for different values of the applied force F (indicated in the figures).

istic force $F_{char} \approx 0.78$ pN, which does not depend on n_t.

At the intermediate forces (0.6 pN $< F < 0.9$ pN) of Fig. 1, we have also observed that the average extension $\langle L_e \rangle$ at negative values of n_t ($n_t < -20$) appears noisier than the data for a positive n_t. We have quantified the fluctuations by calculating the standard deviation of the DNA extension $\sigma_{Le} = \sqrt{\langle L_e^2 \rangle - \langle L_e \rangle^2}$. We have also checked that σ_{Le} was not dependent on the total time of the average and that such time was much longer (more than 100 times) than the characteristic time of the correlation function of the data. The values of σ_{Le} as a function of F for various values of the number of imposed turns n_t are shown in Fig. 2B. An increase in the extension fluctuations σ_{Le} occurs in a narrow range of applied force and presents a maximum value $\sigma_{Le Max}$ around the characteristic force F_{char}: the fluctuations are associated with the denaturation transition. The value $\sigma_{Le Max}$ is an increasing function of $|n_t|$. This is confirmed in the inset of Fig. 2B, where the obtained values of $\sigma_{Le Max}$ are plotted for different values of n_t and show a linear behavior.

We present the same quantities, ΔL_e and σ_{Le}, as a function of n_t for different values of force F (see Fig. 3). We observe that the ΔL_e increase with negative supercoiling starting at $n_t = -10$ (panel A). This transition is not accompanied by an increase in σ_{Le} (panel B). Instead, the strongest fluctuation takes place at the F_{char}, as shown previously.

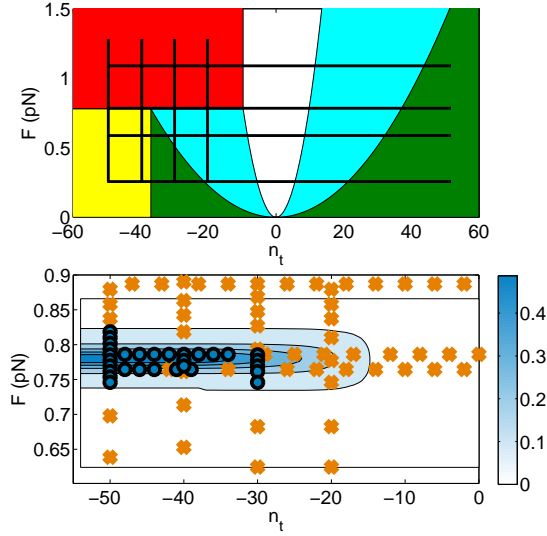We will now present a simple mechanical model that can explain all the experimental findings, quantitatively

FIG. 4: *Panel A*: Calculated phase diagram of DNA structure in the (n_t,F) space. *White*: DNA compatible with the WLC model. *Blue*: plectonemic regions. *Green*: zero DNA extension regions. *Red*: denaturation bubbles region. *Yellow*: coexistence region of denaturation bubbles and plectonemes at zero DNA extension. The vertical and horizontal lines correspond to the measurements presented at constant F (in Fig. 1 and Fig. 3) and at constant n_t (in Fig. 2), respectively. *Panel B* (enlargement of panel A): contour plot of the calculated (*level lines*) σ_{Le}. Crosses (circles) indicate measured values of $\sigma_{Le} < 0.15$ μm ($\sigma_{Le} > 0.15$ μm).

confirming the existence of a fluctuation increase at a characteristic value of the force F_{char} and deriving an original relation between F_{char} and DNA nanomechanical constants (bending constant B and the binding energy between the DNA bases (denaturation energy)). The model is an extension of the classical theory of plectoneme formation [17] considering the denaturation energy. Indeed, when twisted by the magnetic bead, the DNA molecule relaxes the applied work in three different ways: by twisting (twisting energy: E_{twist}), by forming plectonemes (plectonemic energy: E_{plect}) and by partially denaturating (denaturation energy: E_{den}). Accordingly [17]:

$$E_{twist} = \frac{1}{2}\frac{C}{L_0}(2\pi \cdot n_e)^2 \qquad (1)$$

$$E_{plect} = (2\pi R \cdot n_p) \cdot (\frac{B}{2R^2} + F) \qquad (2)$$

while we have evaluated E_{den} as:

$$E_{den} = \alpha \cdot n_d \qquad (3)$$

where L_0 is the contour length of the DNA, n_e is the number of turns that store energy in the twist, n_p is the

number of plectonemes of radius R, n_d is the number of turns relaxed by partial DNA denaturation, C is the twisting constant, and α is a phenomenological constant that will be discussed later. We impose the additional topological relation: $n_e = n_t - n_p - n_d$. Furthermore, we assume that the DNA extension variations are mainly due to the plectoneme formation: $L_e = L_0 - 2\pi R \cdot n_p$. For this assumption, we disregard for the moment the Worm-Like-Chain (WLC) dependence of DNA extension on the applied force and we suppose that the denaturation phenomenon does not induce a significant DNA length variation.

We can estimate the characteristic force F_{char} by using the following back-of-the-envelope calculation. The characteristic force is obtained by equating the plectonemic energy and the denaturation energy which is necessary for relaxing to the same torsion angle (i.e. $\Delta n_p = \Delta n_d$). The value $R = \sqrt{B/2F}$ of the plectonemic radius [17] is kept constant and obtained from the equilibrium of the twisting energy and the plectonemic energy, resulting in the following relations:

$$(2\pi R) \cdot (\frac{B}{2R^2} + F) = \alpha \qquad (4)$$

obtaining for the characteristic force:

$$F_{char} = \frac{\alpha^2}{8B\pi^2} \qquad (5)$$

The parameter α is proportional to the binding energy between the bases of the two DNA single strands. Considering the experimental value $F_{char} \approx 0.78$ pN and a DNA persistence length of about 50 nm, the resulting value of α is on the order of 10^{-19} J, which is consistent with the reported average value of the free energy per DNA base pair, $\Delta G \approx 2.0$ kcal/mole [25–27]. In a first approximation we consider the denaturation energy, described by the average single parameter α, to be independent on the specific DNA sequence. The resulting value of α corresponds to approximately 8 denatured bases to relax one turn. This number of base pairs is consistent with the pitch of the double helix. More rigorously, fixing the external force F and the total imposed torsion n_t, we can study the total energy landscape E_{tot} as a function of the parameters n_p, n_d, and R. By minimizing the expression of the total energy E_{tot} in the (n_t,F) plane, we derive how DNA behaves under imposed torsion and force. The resulting calculations are presented in Fig. 4A where the different colored regions represent different DNA behaviors and the boundary lines correspond to transition lines. In the white central region, the DNA reaches the maximum extension compatible with the applied force according to the WLC model [17]. Entering the lateral blue regions, plectonemic formation starts and DNA extension is consequently reduced. The green regions correspond to achieving zero DNA extension. The novelty of the model is its capability for predicting the denaturation

regions shown in the red (denaturation bubble) and yellow (coexistence regions between plectonemes and bubbles) rectangles. The boundary of each zone corresponds to a transition between different structural phases. We concentrate our attention on the transition to the denaturation state. It is possible to enter the denaturation zone (red and yellow) by crossing three different lines, but only the horizontal line delimiting the red zone is characterized by a step in the DNA extension. Indeed, below this line the DNA has a reduced length due to the presence of several (depending on the turn position) plectonemes and above this line the DNA is fully extended. Accordingly, the fluctuation between the structures configuration is also accompanied by a oscillation in the DNA extension. This feature is unique to this transition; none of the other phase structure boundaries reported in Fig. 4A introduce any discontinuity in L_e.

Furthermore, because L_e depends on n_p, calculating n_p using the proposed expression for the energy E_{tot} and a Boltzmann distribution allows for the prediction of the average value of the DNA extension and its fluctuation σ_{Le}. The calculated values of $\langle L_e \rangle$, corrected for the WLC model, are presented as a function of n_t by the continuous lines in Fig. 1, showing a good agreement with the experimental data. The results are obtained assuming the following values: $B = 1.29 \cdot 10^{-11}$ eV·cm, $C = 3.62 \cdot 10^{-11}$ eV·cm, $L_0 = 1.88$ μm and $\alpha = 0.70$ eV. As shown in Fig. 1, the model accurately describes the classical plectonemic behavior observed for $n_t > 0$, which was already well described in the past [17], as well as the transition between the plectonemic and denaturation regime for $n_t < 0$.

As expected, the region characterized by non-negligible calculated DNA extension fluctuations σ_{Le} is located in a specific area of the plane (n_t, F): at the horizontal boundary of the red zone. This theoretically predicted region is shown as a contour plot in Fig. 4B (enlargement of a region of Fig. 4A). In Fig. 4B we also present, as crosses or circles, respectively, the measured standard deviations having negligible ($\sigma_{Le} < 0.15$ μm) or significant ($\sigma_{Le} > 0.15$ μm) values. From Fig. 4B, we can appreciate the agreement between our model and the experimental results: the regions of largest fluctuation are observed where the model predicts a marginal stability [28] of L_e, i.e., for low n_t value ($n_t \leqslant$ -30) and near the characteristic value of the force $F_{char} \approx 0.78$ pN.

Moreover, in Fig. 4A we sketch vertical and horizontal thick black segments corresponding to the lines explored by the experiments presented in Fig. 2 (fixed n_t) and Fig. 3 (fixed F). As predicted by the model, the asymmetry in L_e indicates entrance into the red zone and large fluctuations appear when crossing the red zone horizontal boundary and when the experiments are performed in its proximity.

In conclusion, we have characterized the denaturation transition caused by external applied force and torsion, and we have introduced a nanomechanical model able to link the measured force at which the denaturation occurs to a parameter α related to the double strand stability. Because DNA denaturation and melting is at the origin of several biological problems ranging from DNA replication and transcription to the detection of transcription initiation points, the ability demonstrated here for a direct, quantitative single molecule measurement of the characteristic force and denaturation energy opens the way for several studies utilizing more sophisticated and biologically realistic situations and in the presence of DNA binding molecules or proteins [29].

[1] C. R. Calladine, H. R. Drew, B. F. Luisi, and A. A. Travers, in *Understanding DNA* (Elesevier Academic Press, San Diego, CA, 2004).

[2] O. C. Lee, J. H. Jeon, and W. Sung, Phys. Rev. E **81**, 021906 (2010).

[3] N. Theodorakopoulos and M. Peyrard, Phys. Rev. Lett **108**, 078104 (2012).

[4] T. S. van Erp, S. Cuesta-Lopez, J. G. Hagmann, and M. Peyrard, Phys. Rev. Lett. **95** (2005).

[5] R. Metzler, T. Ambjornsson, A. Hanke, and H. C. Fogedby, J. Phys. Condens. Matter **21**, 034111 (2009).

[6] C. Nisoli, D. Abraham, T. Lookman, and A. Saxena, Phys. Rev. Lett. **104**, 025503 (2010).

[7] K. C. Neuman and A. Nagy, Nat. Methods **5**, 491 (2008).

[8] T. R. Strick, J. F. Allemand, D. Bensimon, and V. Croquette, Biophys. J. **74**, 2016 (1998).

[9] D. A. Koster, V. Croquette, C. Dekker, S. Shuman, and N. H. Dekker, Nature **434**, 671 (2005).

[10] D. A. Koster, K. Palle, E. S. M. Bot, M. A. Bjornsti, and N. H. Dekker, Nature **448**, 213 (2007).

[11] M. Nollmann, M. D. Stone, Z. Bryant, J. Gore, N. J. Crisona, S. C. Hong, S. Mitelheiser, A. Maxwell, C. Bustamante, and N. R. Cozzarelli, Nat. Struct. Mol. Biol. **14**, 264 (2007).

[12] D. Salerno, D. Brogioli, V. Cassina, D. Turchi, G. L. Beretta, D. Seruggia, R. Ziano, F. Zunino, and F. Mantegazza, Nucleic Acids Res. **38**, 7089 (2010).

[13] J. Lipfert, S. Klijnhout, and N. H. Dekker, Nucleic Acids Res. **38**, 7122 (2010).

[14] J. F. Allemand, D. Bensimon, R. Lavery, and V. Croquette, Proc. Natl. Acad. Sci. U. S. A. **95**, 14152 (1998).

[15] S. B. Smith, L. Finzi, and C. Bustamante, Science **258**, 1122 (1992).

[16] T. R. Strick, J. F. Allemand, D. Bensimon, A. Bensimon, and V. Croquette, Science **271**, 1835 (1996).

[17] T. R. Strick, M. N. Dessinges, G. Charvin, N. H. Dekker, J. F. Allemand, D. Bensimon, and V. Croquette, Rep. Prog. Phys. **66**, 1 (2003).

[18] J. F. Allemand, D. Bensimon, L. Jullien, A. Bensimon, and V. Croquette, Biophys. J. **73**, 2064 (1997).

[19] C. Gosse and V. Croquette, Biophys. J. **82**, 3314 (2002).

[20] J. Lipfert, X. Haoand, and N. H. Dekker, Biophys. J. **96**, 5040 (2009).

[21] A. J. W. te Velthuis, J. W. J. Kerssemakers, J. Lipfert, and N. H. Dekker, Biophys. J. **99**, 1292 (2010).

[22] D. Klaue and R. Seidel, Phys. Rev. Lett. **102**, 028302

(2009).

[23] F. Mosconi, J. F. Allemand, D. Bensimon, and V. Cro-
quette, Phys. Rev. Lett. **102**, 078301/1 (2009).

[24] M. N. Dessinges, B. Maier, Y. Zhang, M. Peliti, D. Ben-
simon, and V. Croquette, Phys. Rev. Lett. **89**, 248102/1
(2002).

[25] K. J. Breslauer, R. Frank, H. Blocker, and L. A. Marky,
Proc. Natl. Acad. Sci. U. S. A. **83**, 3746 (1986).

[26] J. SantaLucia, Proc. Natl. Acad. Sci. U. S. A. **95**, 1460
(1998).

[27] J. M. Huguet, C. V. Bizarro, N. Forns, S. B. Smith,
C. Bustamante, and F. Ritort, Proc. Natl. Acad. Sci.
U. S. A. **107**, 15431 (2010).

[28] D. Brogioli, Phys. Rev. Lett. **105**, 058102 (2010).

[29] I. D. Vladescu, M. J. McCauley, I. Rouzina, and M. C.
Williams, Phys. Rev. Lett. **95**, 158102 (2005).